A. Keller
ETHZ
Zurich
Switzerland

14

Scaling laws with combustion particles

Scaling laws with combustion particles

A. Keller, M. Fierz, K. Siegmann and H.C. Siegmann
Laboratory for Combustion Aerosols and Suspended Particles
Swiss Federal Institute of Technology (ETH)
CH–8093 Zürich, Switzerland

A. Filippov
HTCRE Laboratory and Center for Combustion Studies,
Yale University,
New Haven, CT 065-8286, USA

August 7, 2000

Abstract

The dynamics of nanoparticles in a carrier gas are governed by the physical and chemical nature of the surface. The total surface area can be divided into an "active" and a "passive" part. The "active" surface is the surface on which transfer of momentum, energy and mass from the gas to the particle takes place. The experiments show that the active surface may be determined in physically very different in-situ experiments such as measuring the mobility b, the diffusion constant D, or the mass transfer coefficient K of the particle. The concept of the active surface manifests itself in scaling laws $K \cdot b = \text{const}$, $K \cdot D = \text{const}$ and $Y \cdot b = \text{const}$, found valid over a large range of particle shapes and sizes. Y is the yield of low energy photoelectrons from the particles upon irradiating the carrier gas with light of energy below the ionization energy of the carrier gas molecules but above the photoelectric threshold of the particles. While K and b are independent of the chemical nature of the particles as far as we know today, the simultaneous measurement of Y provides a chemical fingerprint of the particles and allows one to observe, in combination with pulsed lasers as sources of light, the dynamical changes of the active surface while the nanoparticle is interacting with the carrier gas.

1 Introduction

Nanosized liquid or solid bodies may remain suspended in a carrier gas for a long time. They are mesoscopic, containing 10^3-10^6 atoms or molecules, and may exhibit unexpected properties due to their very large surface to volume ratio. Such nanoparticles in a carrier gas have been largely neglected in surface science. Yet it is evident that it would be highly welcome if not urgent to know more about their surface characteristics. Nanoparticles in air, for instance, have moved to the center of attention because of their well documented effect on public health[1]. They are deposited in the alveoles of the lung where the defense mechanisms of the human body are weak; in this way, a number of toxic chemicals adsorbed at the nanoparticle surface penetrate into the human body using the nanoparticles as vehicles. Another example is the precipitation forming process in clouds. It depends to a large extend on the presence of nanoparticles acting as condensation nuclei for ice and water. This has a significant influence on the albedo of the earth and on rain and snowfall[2].

However, none of these phenomena is understood on the atomic level. It is therefore necessary to adapt the techniques developed in surface science to the characterization of the surface of the nanoparticles. It is important to do the investigations while the nanoparticle remains suspended in its carrier gas. Deposition on a substrate and transfer into vacuum may severely alter the surface characteristics of the nanoparticle and, through the action of surface tension, even its

shape. The transfer of momentum, energy, and mass from the gas to the particle as well as the heterogeneous chemical reactions and the surface tension are dominated by an atomically thin layer at the surface. The properties of this layer can be subject to significant transformations without changing the particle bulk parameters. It is well known that a fingerprint of the surface as well as its dynamical changes become observable by measuring the photoelectric yield of the particle while it is suspended in its genuine carrier gas[3]. The surface often depend characteristics on spurious contaminants of the carrier gas and on small changes of the temperature as well as on fine details in the nanoparticle process of production, be it in an internal combustion engine[4] or in a volcano[5]. It is the purpose of this paper to show that surface science with nanoparticles in a carrier gas is possible and a rewarding new field of research with many important applications.

2 Evaluation of the surface area

With nanoparticles it is generally not possible to define the geometry by a few simple parameters, such as diameter, surface area or volume. This arises because nanoparticles may exhibit bizarre shapes with numerous incisions and internal surfaces. But the surface tension may also contract them into perfect spheres, notably if water or other impurities in the carrier gas condense on them, or if the temperature is raised so that the surface atoms become mobile. The electron microscope, in principle a powerful tool to image nanostructures, has its limitations as the nanoparticles may change shape on substrate deposition and on transfer to the vacuum for instance by evaporation of condensates. Yet, one needs to have some measure of the surface area in order to evaluate adsorption and to understand the interaction with the carrier gas.

2.1 The surface area from the mobility or the diffusion constant

The most commonly used technique to determine the "size" of a nanoparticle in-situ relies on the measurement of the mobility b of the particle in its carrier gas. b is defined by assuming a linear friction law $V = b \cdot F$ in which a constant drift velocity V is reached under the action of an external force F. $F = eE$ is generated by attaching one elementary electrical charge e to the particle and bringing it along with the carrier gas into the electrical field E of a condenser. Nanoparticles of one specific b can exit through a slit in the condenser and are counted with a condensation nucleus counter. By scanning the electric field in the condenser and counting the exiting particles at each field strength, the mobility spectrum of the nanoparticles is obtained.

Fig. 1 shows examples of electron micrographs of gold particles that have been generated in an electric discharge between high purity Au-electrodes in Ar-gas which was subsequently heated to the temperature indicated. After that, particles of the mobility $b = 0.92 \times 10^{-3}$ cm^2/(V·sec) were selected, precipitated on a substrate, and imaged in transmission electron microscopy. For the simple case of pure Au-particles in pure argon gas, the aforementioned possible distortions by electron microscopy are minimal. Fig.1 demonstrates that only those particles heated to high temperatures approximate a spherical shape, the diameter of which turns out to be $\approx$ 50 nm. The "nose" of the particle heated to 1300°C is probably due to agglomeration with a smaller particle after the heating section but before the mobility analyzer. The generally accepted function connecting the observed mobility with a particle diameter d_p has been tabulated by N.A. Fuchs[6]. In the case of the particles displayed in Fig. 1, this function yields $d_p = 50$ nm as well. However, the unheated Au-particles have a much larger geometrical surface area compared to the spherical Au particles. The concept of the mobility diameter clearly can be quite misleading. It is outright wrong to derive the area of the geometrical surface or the volume of the particle from it. Correctly, one has to think of d_p as a parameter fixing the "active"-surface which is essentially the part of the surface that causes the friction in the carrier gas as explained below. The "passive" surface includes the inner surfaces and the surface in bays or incisions that does not interact with the carrier gas.

The theory of the friction coefficient $1/b$ of a nanoparticle depends on the Knudsen number $Kn = \lambda/d_p$ where l is the mean free path of the carrier gas molecules; $\lambda = 67$ nm in air at normal conditions. If $Kn \gg 1$, one has the molecular particle motion where the gas molecules fly in vacuo near the particle. The friction coefficient is then caused by the pressure difference between front

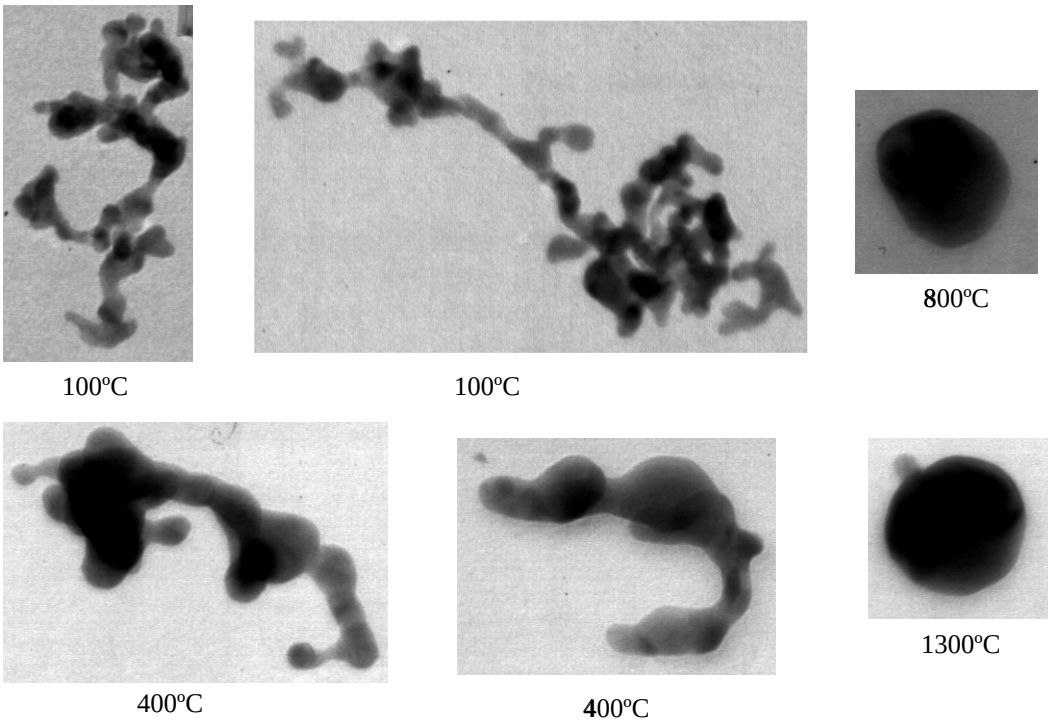

Figure 1: Electronoptical micrographs of gold particles generated in an electric discharge between gold-electrodes. After the generation, the inert carrier gas has been heated to the temperature indicated. The particles have identical mobilities selected in a differential mobility analyzer. This mobility leads to a mobility diameter $d_p = 50$ nm which indeed corresponds to the diameter of the spherical particles heated to 800 and 1300°C. The melting point of bulk gold is 1064°C, but it is obvious that the surface atoms become mobile much below that temperature.

and back of the particle yielding:

$$\frac{1}{b} = \frac{1}{3}\pi n m v \delta d_p^2 \tag{1}$$

where n, m and v are the density, mass, and average velocity of the gas molecules. δ is a factor with value 1.0 or 1.4 depending on whether the reflection of the gas molecules on the nanoparticle is specular or diffuse respectively. Chemically inert surfaces tend to exhibit specular, chemically active surfaces diffuse reflection. In actual aerosol practice, the mode of reflection is assumed to be fixed between these two extremes. In reality, it depends on the accommodation coefficient at the interface gas/particle.

For $Kn \ll 1$, the particle friction is calculated from fluid dynamics. Assuming spherical particles and very small drift velocity one arrives at the Stokes law in which $1/b = \text{const} \cdot d_p$. This is the well known paradoxical result that friction depends only on the diameter, not on the cross section of the moving body as long as one has laminar flow. It can be understood qualitatively by considering that friction is effective on those parts of the surface where the relative velocity between gas and particle drops steeply. This reduces the particle surface active in friction to a small strip around the circumference.

For $Kn \simeq 1$, one has the transition between molecular and hydrodynamic motion. In many practical applications, this is the regime of interest, yet unfortunately the theory has no rigorous foundation there. It turned out that a velocity slip between gas and moving particle must be taken into account, known as the Cunningham correction factor $Cc(\lambda/d_p)$. This function makes it possible to produce a smooth transition between the molecular regime with $1/b \propto d_p^2$ and the hydrodynamic regime with $1/b \propto d_p$. It should be noted that in the molecular regime, $(\pi/4) \cdot d_p^2$ is

the impact cross section averaged over all directions relative to the drift velocity V. This averaging arises because the particle performs a Brownian rotation.

Hence the fraction of the geometrical surface that produces friction continually decreases as Kn decreases, that is as the particle "size" increases. This fraction of the geometrical surface is active in exchanging energy and momentum from the particle to the gas, and we call it therefore the "active" surface. Inner surfaces, and surfaces in bays or cracks, or with the large particles, surfaces around the front and back dead center of the laminar flow are passive surfaces. The "active" surface has also been named "Fuchs"-surface[7].

The diffusion coefficient D of nanoparticles is measured for instance in diffusion batteries[8]. It is inversely proportional to the same active surface as the mobility b at constant temperature T since $D = kTb$, where k is the Boltzman factor.

The mobility and diffusion constant and hence the active surface determines the precipitation of nanoparticles in filters. The larger particle tend to be removed by impaction on obstacles in the carrier gas flow such as hairs. This form of particles deposition is governed by the stopping distance $\lambda_p = VMb$, where M is the mass of the particle. The smaller particles tend to reach the walls of a narrow channel by diffusion according to the deposition parameter $D \cdot (L/Q)$ where L is the length of the channel and Q the volume flow rate of the carrier gas[8]. In the human respiratory tract, for instance, the large particles with a high M are deposited by impaction in the upper part, whereas the small nanoparticles penetrate to the alveoles of the lung were they reach the walls by diffusion.

2.2 The surface area from the mass transfer coefficient

The transfer of molecules of density n from the carrier gas to the nanoparticles of density N describes the growth of the nanoparticles by condensation of gas phase species. If every molecule that hits the particle also sticks to it, the rate of condensation is given by $dn/dt = -KN \cdot n$ where K is the mass transfer coefficient. Obviously the sticking probability is usually < 1. For instance, NO_2 or O_3 have sticking probabilities on carbon nanoparticles of 10^{-4} according to Ref. [9] and [10]. However, electrically charged molecules are reported to transfer at least their charge to any nanoparticle once they contact it. Reactive species such as metal atoms will also bind to any surface. This can be used to measure the mass transfer coefficient K. In the first method, ions are produced in the carrier gas and the electrical charge transferred to the nanoparticles is measured. In the second method that may be applied even with very low densities of nanoparticles, the carrier gas is doped with radioactive lead atoms produced in the decay of the noble gas atom radon. The radioactivity acquired by the nanoparticles provides a measure of K[7]. With a sticking probability of 1, $dn/dt = dN^+/dt$ where N^+ is the density of electrically charged particles or radioactive particles depending on the experiment. This yields

$$N^+ = N_0(1 - \exp(-Ktn_0)) \tag{2}$$

where t is the time of interaction. n_0 and N_0 are the densities of the molecules or atoms and particles at $t = 0$. K has been determined according to eq. (2) by letting the gas carrying the particles interact for a time t with the ions or the radioactive lead atoms, and observing the density N^+ of charged or radioactive particles.

The theory of K depends again on the Knudsen number Kn. For $Kn \gg 1$, the gas molecules fly in vacuo near the particle. The rate with which they hit the particle depends on the averaged particle cross section and the average velocity v of the molecules. This yields

$$K = \frac{\pi}{4} v d_p^2 \tag{3}$$

For $Kn \ll 1$, the continuum theory applies and the molecules with diffusion constant Δ diffuse to the particles. This yields $K = 2\pi\Delta d_p$. Hence just like the friction coefficient $1/b$, K scales with d_p^2 in the molecular regime and with d_p in the macroscopic regime.

At $Kn \simeq 1$, the adsorbing species first have to perform a classical diffusion to the neighborhood of the particle where from the gas kinetics dominate. Some authors have estimated the distance at which this transition occurs, but it turns out, as demonstrated by Filippov[11], that the last

step is best treated in a Monte Carlo calculation of the actual pathways of the molecules. This has the advantage over the older approximations that gas molecule collisions close to the particle are properly taken into account and that even complex interactions such as those occurring between a charged molecule and the image charge induced in the particle can be accounted for in a realistic way. At any rate, again a smooth transition occurs from the macroscopic regime where $K \propto d_p$ to the molecular regime with $K \propto d_p^2$. If it were not for the necessity to assume a sticking probability of 1 in the measurement of K, and a constant mode of reflection of the gas molecules in the case of the mobility b, one might predict from inspecting the theory that at least near the molecular regime, both physically very different experiments depend on the active surface. This implies that a scaling law $K \cdot b =$ const should be valid independently of the particle size. This scaling law must be independent of the actual shape as well as of the chemical nature of the particle.

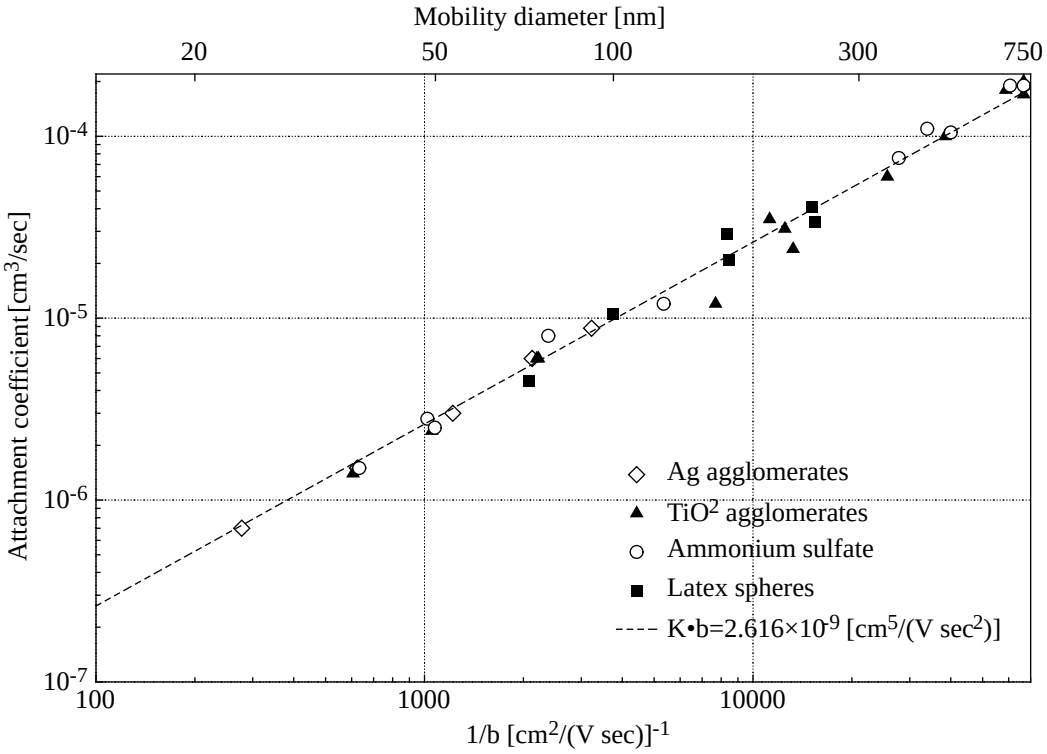

Figure 2: Mass transfer coefficient K plotted against the friction coefficient $1/b$. the mobility diameter d_p as calculated from b is also indicated. The data are adapted from references [12] and [13]. K is determined by attachment of radioactive lead atoms. The carrier gas is air.

Rogak, Baltensperger and Fleagan[12] and Schmidt-Ott et al.[13] measured the mobility b of silver agglomerates, titanium oxide particles and their agglomerates, latex spheres, and ammonium sulphate droplets over a wide range of particle sizes and shapes. Simultaneously, the mass transfer coefficient was also determined using the radioactive lead method. Fig. 2 shows the results of this experiment. K is plotted against the friction coefficient $1/b$. The mobility diameter d_p is calculated from b according to Fuchs[6]. The data extend well over the transition from the macroscopic to the molecular regime, and there is indeed no systematic difference between agglomerates with bizarre shapes and perfectly spherical particles. There is also no difference between metals such as Ag and perfect insulators such as latex spheres which means that the image charge potential is not important. The constant value of $K \cdot b = 2.616 \times 10^{-9}$ [cm^5/Vsec^2] provides a fit to the data. Although there are fluctuations of up to 50% in a single measurement, a systematic deviation for one specific type of particle does not occur. This proves that the active surface determines both K and b, and that both physically very different experiments really measure the same particle property.

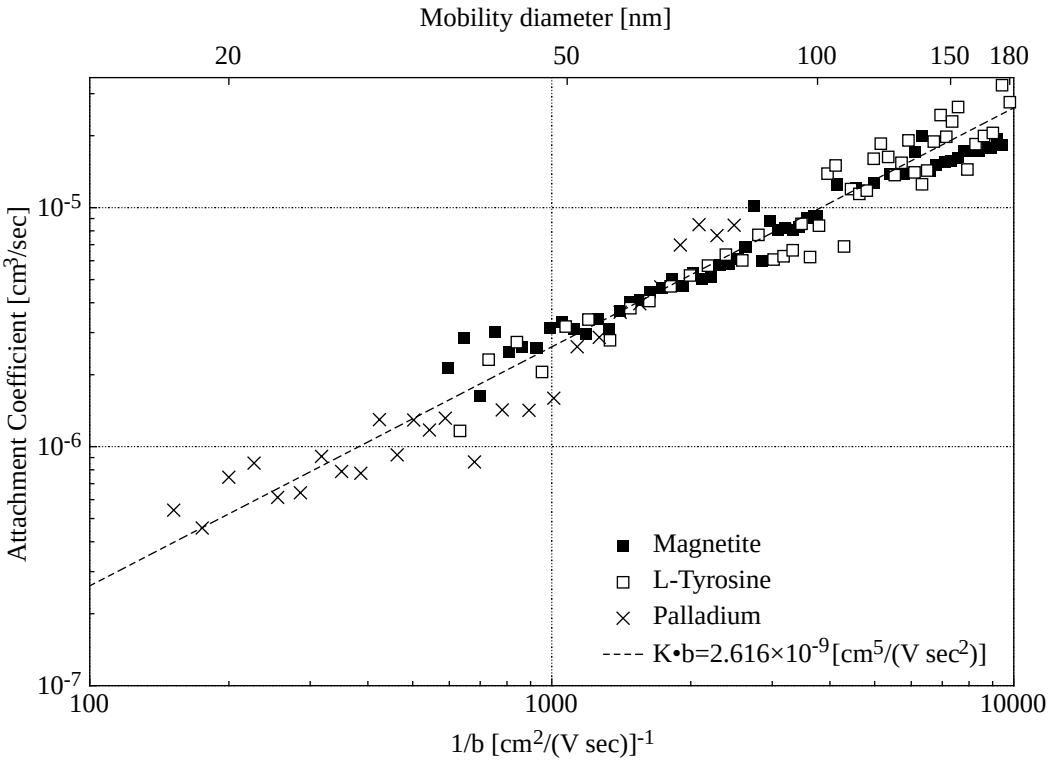

Figure 3: Mass transfer coefficient K versus the friction coefficient $1/b$ for Pd–, Fe_3O_4–, and L–Tyrosine particles. The mobility diameter d_p is also indicated. K is determined by attachment of positive air ions to neutral particles. The carrier gas is air.

Fig. 3 shows results of our own experiments with a large variety of materials ranging from metals to insulators, and from perfect spheres to agglomerates and needle shaped single crystals of the amino acid L-tyrosine. The mass transfer coefficient was determined with the positive air ions produced in a glow discharge. Prior to admitting the carrier gas with the nanoparticles to the region containing the ions, any previously charged nanoparticles were removed by an electrofilter. Again, $K \cdot b = \text{const}$ is verified within experimental uncertainty, and no specific trend can be seen depending on the chemistry or the geometry of the nanoparticles in the range 20 nm$\ll d_p \ll$180 nm. This suggests that the scaling law $K \cdot b = \text{const}$ is universal and also that the concept of the active surface makes sense.

3 The chemical fingerprint of the active surface

The yield Y of photoelectrons with photon energies near photoelectric threshold delivers a fingerprint of the physical and chemical state of the surface of condensed matter, and will depend on optical absorption, that is on bulk properties as well. The advantage of this oldest form of photoelectron spectroscopy is that one can make use of powerful and innovative sources of light such as excimer lamps and pulsed lasers opening up investigations in the time domain as well. The main disadvantage is that threshold photoemission is still poorly understood and in many cases can be interpreted on a phenomenological basis only.

If the sample is immersed in a gas instead of vacuum, the photoelectrons collide with gas molecules, perform a random motion near the sample surface, and eventually diffuse back to it. Therefore, no steady state photoelectric conductivity is observed with macroscopic samples unless one applies an electric field. However, if the dimensions d_p of a particle are small compared to the mean free path λ_e of electrons in the gas, then backdiffusion of the photoelectrons is unlikely. This

occurs with gases at normal conditions for d_p in the nanometer size range. It has been detected by observing photoconductivity with Ag-nanoparticles in air[14]. The condition for this experiment is that the photon energy is below the photoionization energy of the carrier gas, but above the photoelectric threshold of the particles. In the actual practice the photoelectrons are removed by applying an alternating electric field or by letting them diffuse to the walls, and the positive charge left behind on the particles is measured by guiding the gas carrying the particles through a filter in which the particles are precipitated. The electric current flowing to the filter yields the total electric charge carried by the particles.

This simple experiment revealed that some nanoparticles exhibit an extremely large photoelectric yield Y which depends strongly on small amounts of adsorbates. The enhancement of Y with Cu-, Ag-, Au-, Pd-, and Ni-particles of $d_p = 3$ nm in purest He turns out to be 100-fold compared to macroscopic surfaces[15]. At the photon energy $h\nu = 10$ eV, Y approaches unity with Ag-particles in He, that is every incident photon produces almost one photoelectron while the spectral dependence of the yield remains essentially identical to the one observed on bulk Ag[16]. Another remarkable observation is that urban air contains particles with $d_p = 100$ nm with a photoelectric threshold below 5 eV. These particles do not disappear in fog or rain[17] which means that water does not condense on them. It turned out that polycyclic aromatic hydrocarbons (PAH) adsorbed at the particle surface are generating the high photoelectric yield of these particles, in fact, it is possible to determine the density of adsorbed PAH in ambient air by measuring Y[18]. PAH are an issue in public health protection as some species are potent carcinogens, and one knows that they induce lung cancer in humans. The most prominent sources in urban air are diesel vehicles, but every incomplete combustion, be it wood- or coal-fire, or cigarette smoke contributes particles with PAH's adsorbed at the surface. Hence particles with high Y in ambient air invariably point to a nearby combustion source.

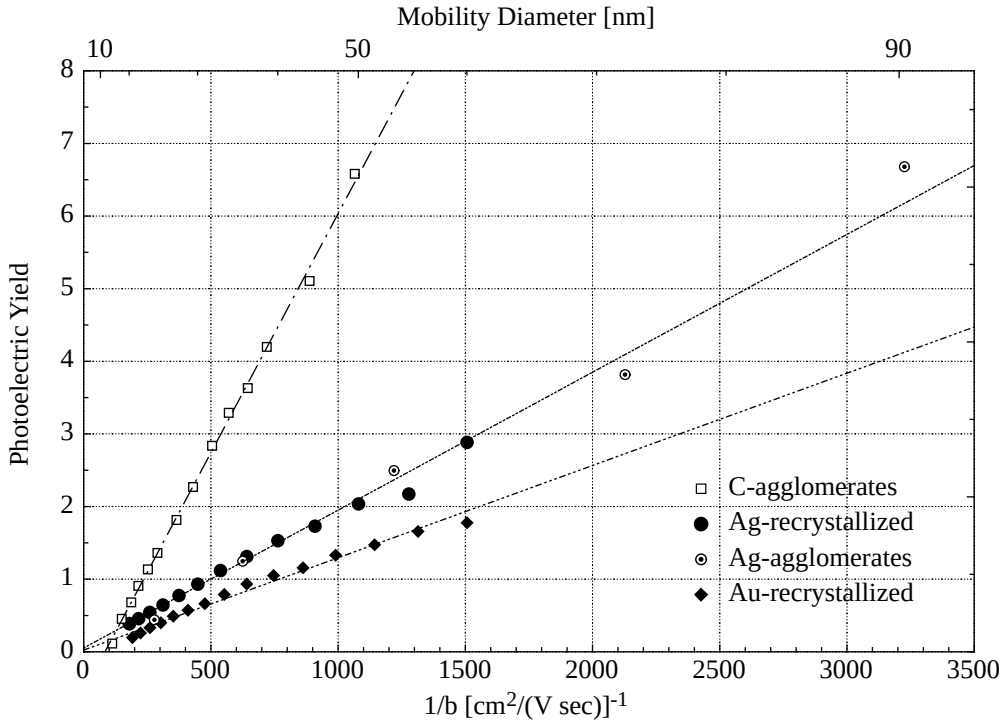

Figure 4: The photoelectric yield Y in arbitrary units vs the friction coefficient $1/b$ for various particles. The data for Ag–agglomerates, and C–agglomerates are from references [13] and [18] respectively, and the recrystallized Ag– and Au–agglomerates are our own measurements. The mobility diameter is also given.

To do proper surface science with nanoparticles, one has to separate the effects on the photo-

electric yield stemming from physical properties such as particle size and surface roughness from the ones induced by the chemical composition of the bulk and at the surface. The window of photon energies useable in photoelectric charging of nanoparticles is narrow; $h\nu$ must be lower than the photoionization energy of the carrier gas but above the work function ϕ of the nanoparticles. In air, one additionally might have to stay below the photon energy inducing excessive ozone formation. Under this condition, $h\nu \geq \phi$, photoelectrons with quite low kinetic energy may be emitted from the surface of the particles into the carrier gas. However, the photoelectron must not be reabsorbed by the particle. It is immediately clear that the inner surfaces will not contribute to photoelectric emission. But the emission from cracks and incisions is not as large as calculated from the geometrical area of the surface because there is a high probability that the emerging photoelectron hits some other part of its parent particle surface and gets reabsorbed. Therefore, it is not surprising that the surface area accounting for the emission of charges from the particle equals the one responsible for the absorption of ions at least in the molecular regime where the ions fly on straight trajectories to the particle. Fig. 4 shows measurements of the photoelectric yield Y plotted against the friction coefficient $1/b$ which is the active surface. The data are for carbon agglomerates[18], silver agglomerates[13], gold agglomerates, and recrystallized Ag- and Au-agglomerates. We see that indeed there is a linear relationship between $1/b$ and Y, but the constant of proportionality does depend on the material and on the photon energy, hence contains the desired chemical fingerprint of the nanoparticle. The physical parameters of particle shape and size can thus be eliminated by a measurement of the mobility b or equivalently a measurement of the mass transfer coefficient K. This is extremely helpful considering the bizarre shapes of the agglomerates shown in Fig. 1. One then has a new scaling law $Y \cdot b = \text{const}$ or equivalently $Y/K = \text{const}$. These laws are important as they show that the chemical fingerprint of the particles may be obtained even with a distribution of particle sizes $N(d_p)$, and without knowledge of the number density. The total photoelectric charge PC carried by the ensemble of particles is

$$PC = \text{const} \int_0^\infty Y \cdot N \, dd_p \tag{4}$$

while the total charge by ion attachment IC is

$$IC = \text{const}^* \int_0^\infty K \cdot N \, dd_p \tag{5}$$

eq. (5) follows from eq. (2) if the product of ion density n_0 and the time t spent in the ion charger is chosen to be low so that $\exp(-Ktn_0) \simeq 1 - Ktn_0$. With $Y = C_1/b$ and $K = C_2/b$ one obtains:

$$\frac{PC}{IC} = CF. \tag{6}$$

CF is a constant that depends only on the photon energy used in PC and on the chemistry of bulk and surface of the particles, hence it delivers "on-line" the desired chemical fingerprint of the ensemble of particles $N(d_p)$ without doing any "size" analysis and without counting the particles. This has been applied for instance to distinguish particles of different origin in automotive exhaust, namely the carbonaceous particles formed in incomplete combustion of the gasoline from the mineralic particles formed out of fuel additives[4]. This is of importance, as the reduction of carbonaceous particle emission is the responsibility of the engine manufacturer, while the particles from contaminants of the fuel are in the responsibility of the gasoline producers. Furthermore, even carbonaceous particles from different types of combustion can be distinguished. This helpful as particles from different combustions carry a different blend of chemicals and therefore pose a different health risk. It turns out, for instance, that a flickering candle produces particles with high CF, while cigarette smoke exhibits an almost 10-times lower CF[19]. Fresh diesel particles are identified readily by their specific CF which is the same all over the world. Diesel particles are the most prominent part of particulate air pollution in major cities like Tokyo and Paris[20]. It is obvious that such techniques, amongst many other applications, will provide a basis for quantifying the health risk imposed by particulate air pollution.

As an example for the observation of the dynamics of the active surface we discuss the measurement of perylene $C_{20}H_{12}$ desorption from graphite particles[21]. An excimer laser delivers pulses

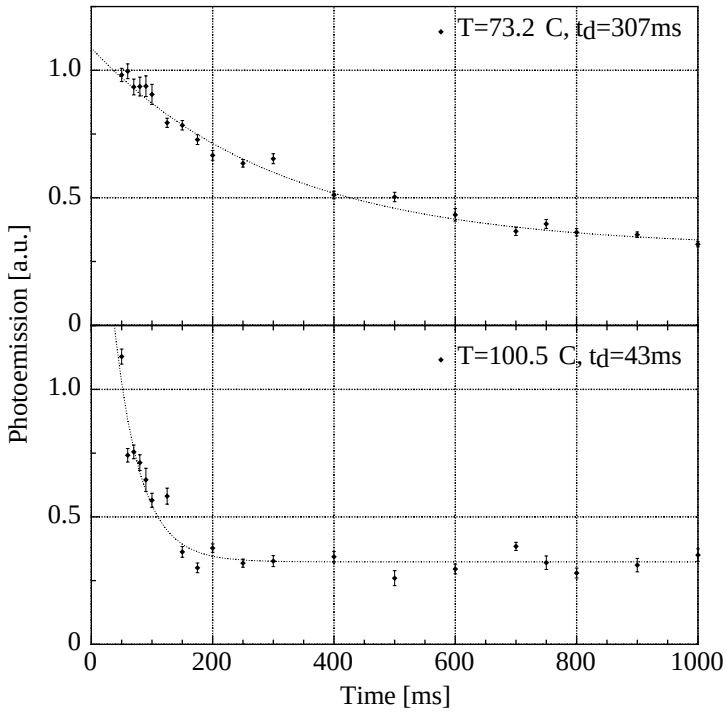

Figure 5: Desorption of perylene from carbon agglomerates of mobility diameter $d_p = 25$ nm at $T = 72.3°$C and $T = 100.5°$C. The dotted lines are exponentials with the time constants $t_d = 307$ msec and $t_d = 43$ msec respectively, from reference [21].

of photons of 6.42 eV energy, the pulse length is 20 nsec. The flat perylene molecule containing 5 aromatic rings was chosen because it stands as a typical representative of the polycyclic aromatic hydrocarbons (PAH) formed in combustion. The well known carcinogen Benzo(a)pyrene is built with 5 aromatic rings as well and should therefore exhibit very similar adsorption/desorption kinetics. In this experiment, the carbon particles are produced in a carrier gas at ambient temperature in which a partial pressure of perylene is maintained. The perylene adsorbs on the particles until an equilibrium between adsorption and desorption is reached corresponding to the density of perylene molecules n_{CH} in the carrier gas and to the number of adsorption sites on the particle. Subsequently a small volume of the gas carrying the perylene loaded particles is transported into the hot carrier gas with $n_{\mathrm{CH}} = 0$ at the temperature $T > T_0$. Now perylene will start to desorb from the particles. The desorption of perylene induces a decrease of the photoelectric yield. After a preset time, the UV laser is fired, and the time dependence of the decrease of Y can be observed by measuring the photoelectric charge on the particles. Fig. 5 shows the time dependence of the desorption for 2 temperatures of the carrier gas. From these measurements, one obtains the adsorption enthalpy of perylene on the particle. The experiment is analog to thermal desorption studies in vacuo, one of the most fruitful techniques in surface science.

Besides source attribution of combustion aerosols[19, 20] and disclosing their surface dynamics as demonstrated in Fig. 5, photoelectric charging of nanoparticles has also been used to study catalytic reaction on soot particles[22]. Furthermore, circular dichroism in the photoionization of nanoparticles built with chiral molecules has also been detected[23]. This makes it possible to distinguish nanoparticles of biological origin from particles synthesized in non-chiral chemical reactions.

4 Theoretical background of the scaling laws

Scaling laws are important in physics as they allow one to generalize the complex phenomena observed for instance in phase transitions. Schmidt-Ott et al.[13] have described scaling laws for mass, surface, and mobility radius of fractal-like agglomerated particles; the term "exposed" surface is used in this work instead of "active" surface employed here. We have given experimental evidence that the following more restricted scaling laws are universal extending to spherical nanoparticles and restructured agglomerates as well. These general scaling laws on changing the particle "size" are: $K \cdot b = \text{const}$, $Y \cdot b = \text{const}$, $K \cdot D = \text{const}$, where b is the mobility, Y the photoelectric yield for threshold photoelectrons, D the diffusion constant of the particles, and K the mass transfer coefficient. We have shown that K may also be determined by simply measuring the electrical charge acquired by neutral particles on adding ions to the carrier gas. We will now discuss some theoretical implications.

The fact that the scaling law $K \cdot b = \text{const}$ is independent on whether the particle is a metal or an insulator demonstrates that the role played by the image force in the approach of an ion is negligible. For conducting particles the image charge potential is largest. The potential energy of ions in an induced image field of a spherical metallic particle with radius a is:

$$U = \frac{1}{4\pi\epsilon_0} \cdot \frac{e^2 a^3}{2r^2(r^2 - a^2)} \tag{7}$$

where e is the elementary charge and r the distance from the particle center. The image charge increases the probability of charging by bending the trajectories of passing ions towards the particle. This is estimated to be significant if U becomes comparable to the average ion kinetic energy $E_k = 3/2kT$ at distances from the particle surface of the order of the particle radius. For example, equating U and E_k at $r^2 = 2a^2$ one obtains an estimate for the critical particle size below which the image charge potential should become important:

$$a_{\text{cr}} = \frac{1}{4\pi\epsilon_0} \cdot \frac{e^2}{6\kappa T} \tag{8}$$

This yields $d_p = 2a_{\text{cr}} \simeq 20$ nm. The present measurements displayed in Fig. 3 extend only to $d_p \geq 20$ nm. At lower mobility diameters, one should observe an increase in $K \cdot b$ depending on $\varepsilon(\omega)$, the frequency dependent dielectric constant of the particle. This increase, if it can be observed, might provide a new test of the electronic properties of mesoscopic matter. Such information is urgently needed in cluster science, for instance to better understand the elusive nature of cloud condensation nuclei[24].

Due to the absence of a theory for the mobility b in the transition between molecular and hydrodynamic motion of the particle, there is no rigorous proof for $K \cdot b = \text{const}$. However, formulae that are tested empirically exist for both K and b[25, 6]. Sherman[26] found that existing experimental data can be adequately described by the empirical formula

$$\frac{q}{q_c} = \frac{1}{1 + q_c/q_f}, \tag{9}$$

where q, q_c and q_f are the transfer rates in the transition, continuum and free–molecular regime, respectively. Correspondingly, for the mass transfer coefficient we have[25]

$$\frac{K}{K_c} = \frac{1}{1 + \sqrt{\pi} Kn}, \tag{10}$$

where K_c is the continuum–regime mass transfer coefficient.

Similarly, using the Cunningham correction factor[25] for the particle mobility we obtain:

$$\frac{b}{b_c} = 1 + Kn\,[A_1 + A_2 \exp(-A_3/Kn)] \tag{11}$$

where b_c is the particle mobility in the continuum limit and the values of the constants can be taken as $A_1 = 1.257$, $A_2 = 0.4$ and $A_3 = 1.1$. The last two equations yield:

$$Kb = K_c b_c \frac{1 + Kn\,[A_1 + A_2 \exp(-A_3/Kn)]}{1 + \pi^{1/2}} \tag{12}$$

This equation predicts that the product $K \cdot b$ can vary only slightly, within 14%, as Kn increases from 0 to infinity. The deviations are largest for $Kn = 1$. This region should be tested carefully to find out whether this deviation is real or an artifact of the interpolation schemes. It also might be possible that with an inert carrier gas and non-passivated surfaces, the scaling breaks down due to different reflection modes of the carrier gas molecules at the particle surface. Plotting $K \cdot b$ is the most obvious way to detect such an effect if it exists.

The scaling laws containing the photoelectric yield Y, namely $Y \cdot b = \text{const}$, $Y/K = \text{const}$, $Y \cdot D = \text{const}$, so far have only been tested for particles with $d_p < 100$ nm. For larger particles with $d_p > 200$ nm, the onset of classical diffusion leads to back-diffusion of the photoelectric charges to the particle. According to Filippov, Schmidt-Ott and Fendel[27], the probability p_e of liberation of a photoelectric charge is given by

$$p_e = \left(1 + \frac{3}{4Kn_e}\right)^{-1} \tag{13}$$

$Kn_e = \lambda_e/d_p$ is the Knudsen number for the free electrons with λ_e the mean free path of low energy electrons in the carrier gas. In air it takes many collisions before the free electron attaches itself to O_2 and produces the negative ion O_2^-. In N_2-gas, no negative ions are formed and $\lambda_e = 670$ nm at normal conditions. It is assumed that this value for λ_e also applies to air. Eq (8) yields then $p_e \simeq 0.5$ for $d_p = 500$ nm, while $p_e = 1$ for $Kn_e \gg 1$ (small particles) and $p_e = 0$ for $Kn_e \ll 1$ (large particles in the micrometer range). The photoelectric yield of a particle is given by $Y = (\pi/4)d_p^2 y p_e$ where y is the yield per unit area of the active surface. The effective specific yield $y \cdot p_e$ decreases as the particle increases but at a different rate compared to the active surface responsible for the friction coefficient $1/b$. It is therefore not expected that the scaling laws containing Y are valid for larger particles approaching the micrometer range. Yet this still waits detailed experimental and theoretical investigation.

5 Conclusion

Surface characteristics of mesoscopic condensed matter or nanoparticles can be evaluated while the particles are suspended in a carrier gas. There are three physically very different experiments to determine the area of the "active"-surface, namely the measurement of the mass transfer or attachment coefficient K, the mobility b, and the diffusion constant D. Combining one of these experiments, preferably the attachment of positive gas ions to the particles with photoelectric charging makes it possible to obtain a chemical fingerprint of the particles without knowing their number or their sizes. It amounts to separating the effects of the physical shape and size of the sometimes bizarre agglomerates from their chemistry. This arises because ion attachment determines the total area of the active surface of the ensemble of particles while photoelectric emission of low energy electrons is also proportional to the same active surface but additionally contains a factor depending on the chemical nature of the particles. By choosing the appropriate light source, one can be highly sensitive to a specific adsorbate/particle system. Using pulsed lasers, it will be possible to observe the surface dynamics down to the femtosecond time scale.

The empirical scaling laws $K \cdot b = \text{const}$, $Y \cdot b = \text{const}$, $Y \cdot D = \text{const}$ and $Y/K = \text{const}$ connect different phenomena such as particle friction, surface growth by condensation of gas phase species, particle diffusion to a wall, attachment of gas ions, and the photoelectric yield Y. The scaling laws are extremely helpful for comparison and calibration of instruments based on very different physical principles. Possible deviations from the scaling laws might turn out to yield additional information on the particles, for instance concerning their dielectric properties, or the mode of reflection of the carrier gas molecules on the surface.

The scaling laws point to the importance of the "active" surface which has also been termed "Fuchs" surface[7] and "exposed" surface[13]. The active surface determines the rate of particle growth by surface condensation, the ultimate speed of chemical reactions involving the carrier gas, and the catalytic activity. The active surface also determines the deposition of particles by impaction and by diffusion in particle filters. For example, knowing the active surface one can predict particle deposition in the inner and outer human respiratory tract. Therefore, the active

surface is one of the most important physical properties of nanoparticles in a carrier gas and should be chosen in the future to characterize nanoparticle air pollution. Surface science with nanoparticles in a carrier gas is a young field with excellent chances for further growth and numerous important applications.

References

[1] Annette Peters, Jiri Skorkovsky, Frantisek Kotesovec, Jaromir Brynda, Claudia Spix, H. Erich Wichmann, and Joachim Heinrich. *Enviromental Healt*, 108(4):283–287, 2000. And references cited therein.

[2] D. Rosenfeld. *Science*, 287:1793–1796, 2000. And references cited therein.

[3] M. Kasper, A. Keller, J. Paul, K. Siegmann, and H.C. Siegmann. *J. of Elec. Spec.*, 98–99:83–93, 1999.

[4] U. Matter, H.C. Siegmann, and H. Burtscher. *Enviromental Science and Technology*, 33:1946–1952, 1999.

[5] M. Ammann, R. Hanert, H. Burtscher, and H.C. Siegmann. *J. of Goephys Res.*, 98:551–556, 1993.

[6] N.A. Fuchs. *The Mechanics of Aerosols*. Dover Publ. Inc., New York, 1964.

[7] H.W. Gäggeler, U. Baltensperger, M. Emmennegger, D.T. Jost, A. Schmidt-Ott, P. Haller, and M. Hofmann. *J. Aerosol Sci.*, 20:557–564, 1989.

[8] William C. Hinds. *Aerosol Technology*. John Wiley & Son, 1982.

[9] M. Kalberer, M. Ammann, K. Tabor, Y. Parrat, E Weingartner, D. Piguet, E. Rössler, D.T. Jost, A. Türler, H.W. Gäggeler, and U. Baltensperger. *J. Phys. Chem.*, 100:15487, 1996.

[10] W. Fendel, D. Matter, H. Burtscher, and A. Schmidt-Ott. *Atmos. Environ.*, 29:967, 1995.

[11] A.V. Filippov. *J. of Aerosol Sci.*, 24:423–436, 1993.

[12] S.N. Rogak, U. Baltensperger, and R.C. Fleagan. *Aerosol Science and Technology*, 14:447–458, 1991.

[13] A. Schmidt-Ott, U. Baltensperger, H.W. Gäggeler, and D.T. Jost. *J. of Aerosol Sci.*, 21:711–717, 1990.

[14] A Schmidt-Ott, P. Schurtenberger, and H.C. Siegmann. *Phys. Rev. Lett.*, 45:1284–1287, 1980.

[15] B. Schleicher, H. Burtscher, and H.C. Siegmann. *Appl. Phys. Lett.*, 63:1191, 1993.

[16] U. Chüller, H. Burtscher, and A. Schmidt-Ott. *Phys. Rev. B*, 38:7814, 1988.

[17] H. Burtscher and H.C. Siegmann. *Combustion Sci. and Technology*, 101:327, 1994.

[18] H. Burtscher. *J. of Aerosol Sci.*, 23:549–595, 1992.

[19] K. Siegmann, L. Scherrer, and H.C. Siegmann. *J. of Molecular Structure (Theochem)*, 458:191–201, 1999.

[20] Q. Zhiqiang, K. Siegmann, A. Keller, U. Matter, L. Scherrer, and H.C. Siegmann. *Atmospherical Environment*, 34:443–451, 2000.

[21] Ch. Hueglin, J. Paul, L. Scherrer, and K. Siegmann. *J. Phys. Chem. B*, 101:9335–9341, 1997.

[22] M. Kasper, K. Sattler, K. Siegmann, U. Matter, and H.C. Siegmann. *J. of Aerosol Sci.*, 30:217–225, 1999.

[23] J. Paul and K. Siegmann. *Chemical Physical Letters*, 304:23–27, 1999.

[24] Markku Kulmala. *J. of Aerosol Sci.*, Supl. 1:1–2, 1999.

[25] M.M.R. Williams and S.K. Loyalka. *Aerosol Science: Theory and practice*. Pergamon Press, 1991.

[26] E. Sherman. In *III Int. Symp. on Rarefied Gas Dyn.*, volume II, pages 228–260, 1963.

[27] A.V. Filippov, A. Schmidt-Ott, and W. Fendel. *J. of Aerosol Sci.*, 24(Suppl. 1):S501–S502, 1993.